Open Access Library Journal
2026, Volume 13, e14798
ISSN Online: 2333-9721
ISSN Print: 2333-9705

Research Paper on the Design and Motion Control of Bionic Mechanical Insects

Yingxin Zhang, Yuxuan Zhang, Meiqi Yin

College of Humanities, Zhejiang Normal University, Jinhua, China
Email: 2823381181@qq.com

How to cite this paper: Zhang, Y.X., Zhang, Y.X. and Yin, M.Q. (2026) Research Paper on the Design and Motion Control of Bionic Mechanical Insects. *Open Access Library Journal*, **13**: e14798.
https://doi.org/10.4236/oalib.1114798

Received: December 22, 2025
Accepted: January 18, 2026
Published: January 21, 2026

Abstract

In the field of micro-robotics, biomimetic robotic insects, with their miniaturized size, high-efficiency locomotion, and strong environmental adaptability, hold irreplaceable value in critical applications such as disaster search and rescue, precision equipment inspection, and military reconnaissance. Current research on biomimetic robotic insects commonly faces core challenges, including insufficient efficiency in miniaturized actuation, poor stability of movement in complex environments, and imbalances between control precision and computational capacity. This paper takes the cockroach as a biological prototype and systematically conducts research on the design and motion control of biomimetic robotic insects. The core research content includes: modeling the motion characteristics of the biological prototype, lightweight structural design and optimization, development of a novel actuation system, and the design of intelligent motion control strategies. Employing a combined research methodology of high-speed video motion capture, finite element analysis, simulation modeling, and physical testing, this study innovatively designs a micro-actuation system based on flexible hinge transmission and proposes a lightweight control architecture integrating model predictive control with deep learning. Prototype test results demonstrate that the designed biomimetic robotic insect, with a body length of 2 cm and a weight of 1.8 g, achieves off-line crawling at a speed of 35 cm per second, maintains stable movement while carrying five times its own body weight, and possesses the capability to traverse complex obstacle environments. The research outcomes provide an effective technical solution for enhancing the locomotion performance and environmental adaptability of micro biomimetic robots, holding significant theoretical reference and engineering application value.

Subject Areas

Mechanical Engineering

Keywords

Bionic Mechanical Insects, Structural Design, Flexible Actuation, Motion Control, Deep Learning

1. Introduction

1.1. Research Background and Significance

With the rapid advancement of micro-electro-mechanical systems (MEMS) technology, the application of micro-miniature robots in extreme environment exploration, civil rescue, and national defense security has become increasingly urgent. Traditional wheeled and tracked micro-robots face significant limitations in navigating confined spaces and adapting to complex terrains. In contrast, insects, having evolved over hundreds of millions of years, have developed highly efficient locomotion mechanisms and exceptional environmental adaptability tailored to the micro-scale. For instance, cockroaches navigate rock crevices with agility, while bees execute precise aerial maneuvers [1]. These biological traits provide natural bionic blueprints for micro-miniature robot design.

As a vital branch of micro-miniature robotics, bio-inspired mechanical insects leverage their core advantage: translating insect biology into engineering solutions to achieve miniaturized, lightweight, and highly efficient motion. In practical applications, these robots can inspect jet engine interiors for defects, conduct life-saving searches in earthquake rubble, or perform covert environmental reconnaissance—effectively filling gaps left by conventional robotic technologies.

However, as robot dimensions shrink to centimeter or even millimeter scales, conventional drive and control schemes face severe challenges: achieving efficient power delivery within confined spaces while ensuring motion stability and control precision has become a critical bottleneck constraining the development of biomimetic mechanical insects. Therefore, conducting research on the structural design and motion control of biomimetic mechanical insects holds significant theoretical value and engineering significance for overcoming the bottlenecks in micro-miniature robotics technology and expanding its cross-domain applications.

1.2. Current Research Status at Home and Abroad

International research in biomimetic mechanical insects began earlier and has achieved a series of breakthroughs. A team from the Massachusetts Institute of Technology (MIT) developed an aerial micro-biomimetic robot. Utilizing flexible artificial muscles to drive biomimetic wings and employing a real-time control strategy based on deep learning, it achieved highly maneuverable actions, including performing 10 consecutive forward somersaults within 11 seconds. Its flight speed and acceleration surpassed previous systems by more than fourfold. The robot's dual-layer control architecture—combining a model predictive controller with a lightweight strategy network—effectively mitigates the trade-off between

computational power and performance at the micro-scale. Harvard University's RoboBee series, driven by piezoelectric ceramic actuators, enables millimeter-scale controllable flight and underwater movement, laying the foundation for multi-modal motion in biomimetic robots.

Domestic research has advanced rapidly in recent years with notable achievements. After 15 years of continuous R&D, Beihang University developed the BHMbot biomimetic insect robot. Measuring 2 cm in length and weighing 1.76 g, it employs a linear drive and flexible hinge transmission system, eliminating reliance on traditional motors and external wires. It achieves wireless autonomous crawling at 37 cm/s and maintains high-speed movement even under loads reaching 5.5 times its body weight. It maintains high-speed movement even under loads reaching 5.5 times its own mass and has demonstrated strong application potential in scenarios such as internal inspection of aircraft engines and patrols in confined spaces. Additionally, research institutions including Tsinghua University and Harbin Institute of Technology have achieved significant breakthroughs in areas like bionic structural topology optimization and high-performance actuator design.

Despite these phased achievements in domestic and international research, current bionic mechanical insects still face three core challenges:

Low energy efficiency in micro-actuator systems limits endurance, with most prototypes still requiring external power or offering only brief operational windows;

Insufficient adaptability to complex, unstructured environments, with significantly reduced stability on irregular terrains such as slopes and soft ground;

Control strategy robustness requires improvement, as precision and reliability become difficult to guarantee when confronting manufacturing tolerances and external disturbances.

These issues form the key focus of this research and represent the technical bottlenecks that must be overcome to advance the field from laboratory prototypes to practical applications.

1.3. Research Content and Technical Approach

This study follows a comprehensive workflow for biomimetic mechanical insects: "biological modeling → structural design → drive development → control implementation → experimental validation" [2]. Core components include:

Using cockroaches as biological prototypes, conducting morphological structure and motion characteristic analyses to establish high-precision kinematic and dynamic models;

Designing lightweight, high-strength biomimetic structures—including the body, leg joints, and foot structures—based on the biological model, and optimizing them through finite element analysis;

Developing efficient micro-scale drive systems, encompassing drive unit selection, flexible transmission mechanism design, and drive circuit development;

Designing robust motion control strategies, constructing a hierarchical control

architecture, and developing gait generation and posture stabilization algorithms integrating model prediction with deep learning;

Construct prototypes and conduct performance testing to validate the feasibility and superiority of the design solutions.

The technical approach is as follows: First, capture cockroach motion data using high-speed cameras and motion capture systems to establish a biological motion model. Based on this model, design structural and drive system solutions, utilizing 3D modeling and finite element analysis software for optimization. Subsequently, build prototypes, develop control programs, and conduct simulation debugging. Finally, establish an experimental platform to test motion performance, load-bearing capacity, and environmental adaptability under various conditions, refining the design based on test results.

The core challenges of this research include: balancing drive efficiency and structural strength at the micro-scale, controlling motion stability in complex environments, and achieving lightweight control architectures. To address these challenges, flexible transmission technology will enhance drive efficiency, deep learning algorithms will improve control robustness, and material selection combined with structural optimization will ensure lightweight and strength requirements.

2. Biological Prototypes and Modeling Analysis of Bionic Mechanical Insects

2.1. Selection and Characterization of Biological Prototypes

The selection of biological prototypes requires comprehensive consideration of locomotive performance, structural complexity, and miniaturization feasibility. This paper adopts the common German cockroach (Blattella germanica) as the biomimetic prototype, primarily based on the following criteria: First, it possesses outstanding locomotive capabilities. Despite its compact size (body length 1 - 2 cm), the German cockroach achieves high-speed crawling, rapid turning, and obstacle crossing, with a stride frequency reaching dozens of times per second, adapting to diverse ground environments; Second, its relatively regular structure. The body is divided into head, thorax, and abdomen. The thorax bears three pairs of well-defined legs, each comprising multiple segments including the basal segment, trochanter, femur, tibia, and tarsus, facilitating engineering modeling and replication. Third, its outstanding load-bearing capacity. The German cockroach can carry objects several times its own weight, providing crucial reference for load design in biomimetic robots.

Observation and analysis using a stereomicroscope confirmed that the German cockroach's primary locomotive organs are its three pairs of thoracic legs. Each leg forms a multi-degree-of-freedom kinematic chain: the forelegs primarily guide and support, while the middle and hind legs provide the main propulsive force. Claw-like structures at the leg tips significantly enhance ground adhesion. Their flattened body shape facilitates navigation through narrow spaces, while their exoskeleton, composed of lightweight chitinous material, balances structural strength

with minimal weight.

Further quantitative testing of its locomotion characteristics was conducted using a high-speed camera system (capturing at 200 fps). When traversing flat surfaces, the German cockroach employs a typical triangular gait pattern. It forms a support triangle using the forelegs and the opposite hind legs, alternating between support and swing phases to achieve stable crawling. Test results indicate an average crawling speed of 30 cm/s (approximately 150 times its body length). Turning is achieved by adjusting the stride frequency and stride length difference between the left and right legs, with a turning response time of less than 0.1 seconds. In obstacle-laden environments, the German cockroach actively modulates its leg movement trajectories, successfully navigating barriers 1.5 times its own height, demonstrating exceptional adaptability to unstructured environments.

2.2. Modeling Biological Kinematics

Based on biological observation data, a leg kinematic model for the German cockroach (Blattella germanica) was established. The D-H parameter method was employed to model a single leg, constructing forward kinematic equations with joint angles as inputs and terminal foot positions as outputs. High-speed camera recordings captured angular changes at each leg joint. Least squares fitting was used to establish the functional relationship between joint angles and time, yielding mathematical expressions for the leg motion trajectory. [3] Experimental measurements revealed the following joint angle ranges during the swing phase of the German cockroach's mesopod: - Tarsomere-proximal segment joint: 30˚ - 60˚ - Proximal segment-femur joint: 45˚ - 90˚ - Femur-tibia joint: 60˚ - 120˚ These data determined the degrees of freedom and motion ranges for the biomimetic leg joints. (See Figure 1)

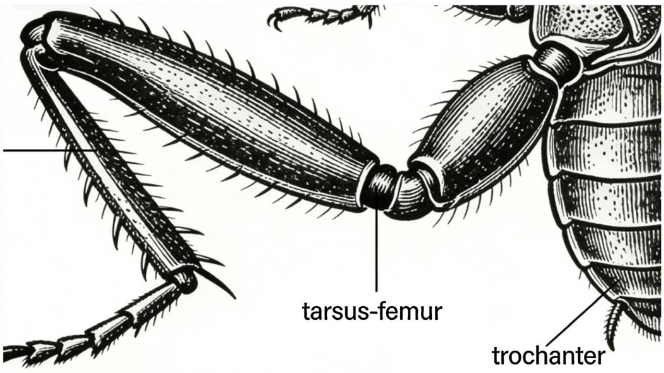

Figure 1. Insect leg segments: trochanter, femur, tarsus.

Dynamic modeling requires consideration of body-environment interactions. A multibody dynamics model was established using Lagrange equations. External loads including ground reaction forces, friction, and air resistance were incorporated into the model. Drive torque was set as the input, while body motion states (velocity, acceleration, attitude angles) served as outputs. A dynamic simulation

model was constructed using ADAMS simulation software. Measured joint motion data were input to validate the model's accuracy. Simulation results showed less than 5% deviation from experimental data, confirming the model accurately reflects the German cockroach's locomotion mechanism.

To validate the reliability of the modeling results, a motion capture system was employed to reconstruct the three-dimensional trajectory of the German cockroach's crawling process. Markers were affixed to key joints on the legs (See Figure 2), and synchronized multi-camera filming captured the three-dimensional coordinate data of these markers. This data was then compared with the predicted trajectory from the kinematic model. Results showed over 92% trajectory overlap between the two, confirming the model's validity and providing accurate biological basis for subsequent biomimetic design and control strategy development.

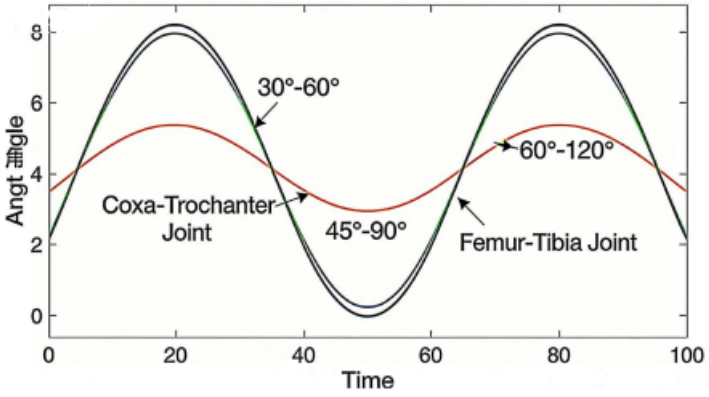

Figure 2. Insect leg joint angle vs. time.

2.3. Extraction of Core Bionic Design Principles

Based on biological prototype analysis and modeling, three key design principles for bionic mechanical insects were identified: First, the miniaturization principle requires prototype dimensions to be confined within 2 cm × 1 cm × 0.5 cm and weight below 2 g. This is achieved through lightweight materials and compact layout to ensure navigability in confined spaces. Second, the principle of motion efficiency: drawing inspiration from cockroaches' triangular gait and high-frequency movement characteristics, designing multi-degree-of-freedom leg structures and efficient transmission systems to achieve a target crawling speed of no less than 30 cm/s and a step frequency of 200 steps/second. Third, the principle of environmental adaptability: enhancing ground adhesion through biomimetic foot structures and optimizing leg movement trajectories to ensure stable movement on slopes, rough surfaces, and obstacle-laden environments.

3. Structural Design and Optimization of Bionic Mechanical Insects

3.1. Overall Structural Design

The body adopts a three-module design comprising head, thorax, and abdomen.

The head integrates control and communication modules, the thorax houses drive units and leg connection structures, while the abdomen accommodates the power supply module. Material selection prioritizes lightweight yet structurally robust high-strength carbon fiber composites for the body shell, while 3D-printed polylactic acid (PLA) is used for leg structures due to its excellent formability and cost-effectiveness. The entire structure is modeled in SolidWorks using a flattened layout, with body thickness controlled below 0.5 cm to accommodate narrow-space operations.

The leg structure underwent bionic optimization based on the biokinematic model of the German cockroach. Each leg features three rotational degrees of freedom (proximal segment-metatarsus, metatarsus-femur, femur-tibia), with optimized link lengths ensuring terminal trajectories closely mimic the biological prototype's movement characteristics. Specific link dimensions are based on measured data: basal segment 2 mm, trochanteric segment 1.5 mm, femur 3 mm, tibia 2.5 mm, tarsus 2 mm. Legs connect to the body via flexible hinges, effectively reducing motion impact and friction loss.

The drive and sensing system adheres to compact layout and lightweight principles: six miniature drive units are symmetrically arranged on both sides of the chest, independently controlling the movement of three pairs of legs. The head houses an STM32 microcontroller, a Bluetooth module, and an Inertial Measurement Unit (IMU), with the IMU continuously capturing the body's three-axis acceleration and angular velocity. The abdomen carries a 3.7 V/100 mAh miniature lithium battery, providing sustained power support for the entire system. The overall layout was validated in the SolidWorks motion simulation environment, ensuring no component interference and a stable center of gravity that meets balance requirements during dynamic movement.

3.2. Key Component Design

Leg joints employ a rotary joint structure. To minimize friction and enhance motion precision, a clearance fit design is adopted with clearance controlled within 0.02 mm. Joint shafts are made of stainless steel with a diameter of 0.5 mm, laser-cut to ensure dimensional accuracy. Joint housings and connecting rods are 3D-printed as monolithic parts to eliminate assembly errors. To enhance load-bearing capacity, miniature bearings are installed at the joints, improving motion smoothness and service life.

Connecting components utilize a composite "snap-fit + adhesive bonding" method. Modules are rapidly assembled and disassembled via snap-fit structures for easy maintenance and debugging. Critical load-bearing areas are reinforced with high-strength adhesives to ensure structural integrity. Legs connect to the drive unit via keyed joints, with keyway dimensional accuracy controlled to ±0.01 mm for reliable power transmission.

The foot structure employs a biomimetic design inspired by the claw-like structure and bristle characteristics of cockroach feet, featuring a "dual-claw + anti-slip

texture" configuration. Two symmetrical claw-like protrusions are positioned at the foot tips, angled at 60˚ to enhance grip on rough surfaces (See Figure 3). Micron-level anti-slip textures are machined onto the sole surface to increase friction against smooth surfaces. Static friction tests demonstrate that the bionic foot achieves a 60% higher coefficient of friction on glass surfaces compared to a flat foot, significantly improving the prototype's ground adaptability.

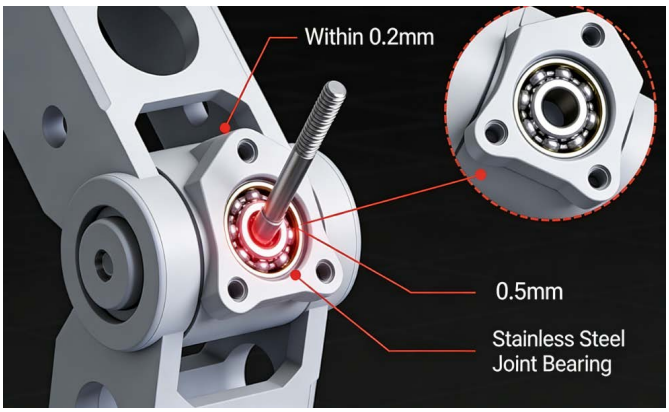

Figure 3. CoreSphere.

3.3. Structural Optimization Analysis

Structural strength optimization of the body was performed using ANSYS finite element analysis software. A finite element model of the body was constructed, subjected to equivalent loads (including self-weight, drive unit weight, and maximum external load), and the structural stress distribution was systematically analyzed. Simulation results revealed significant stress concentration at the shoulder-to-leg junction, with peak stresses exceeding the material's allowable limit. To address this, the structural design was optimized by adding 0.2 mm-thick stiffeners to the critical area. Post-optimization, maximum stress decreased by 45%, meeting strength requirements [4].

To enhance motion flexibility, leg movement interference was optimized. Using ADAMS motion simulation software to model the leg's trajectory throughout a complete cycle revealed minor interference between the midfoot and hindfoot during the swing phase. By adjusting the leg mounting angles—advancing the midfoot mounting position by 1 mm and retracting the hindfoot by 1 mm—the design underwent re-simulation. Following optimization, the motion interference was completely eliminated. Concurrently, joint clearances were optimized and solid lubricants applied to joint surfaces, effectively reducing friction and improving leg flexibility by 30%.

To enhance miniaturization feasibility, the transmission chain and structural complexity were prioritized for optimization. A direct connection design between the drive unit and leg joints eliminated intermediate transition gears, shortening the transmission chain by 2 mm. Concurrently, a highly integrated design merged the control chip and communication module into a single unit, reducing the cir-

cuit board area by 30%. Through these optimization measures, the final prototype weighs 1.8 g with dimensions of 2 cm × 1 cm × 0.45 cm, meeting miniaturization design criteria.

3.4. Prototype Fabrication and Assembly

Manufacturing processes were selected based on component characteristics: the body shell utilized carbon fiber prepreg compression molding to ensure structural strength and surface precision; complex components like legs and joints employed photopolymerization 3D printing with 0.01 mm accuracy to precisely realize intricate designs; circuit boards for drive units and control modules were fabricated via PCB photolithography to guarantee stable electrical performance.

The assembly process follows the principle of "inside before outside, bottom before top": First, the drive units and circuit boards are assembled onto the chest frame, with electrical connections completed and tested. Next, the leg structures are installed, with joint clearances and ranges of motion adjusted to ensure smooth leg movement. Subsequently, the head and abdominal modules are assembled, with power and communication lines connected. Finally, comprehensive debugging is performed to verify assembly precision and movement coordination across all components. During assembly, microscopes are used for positioning assistance, ensuring critical assembly precision within 0.02 mm.

Prototype basic parameter test results are as follows: weight 1.8 g, dimensions 20 mm × 10 mm × 4.5 mm, leg movement degrees of freedom 3 × 6 = 18 (See Figure 4), body center of gravity height 2 mm, meeting design requirements. Through degree-of-freedom verification testing, the range of motion for each joint conformed to design values with no sticking phenomena, achieving the expected goals for overall structural reliability and movement flexibility.

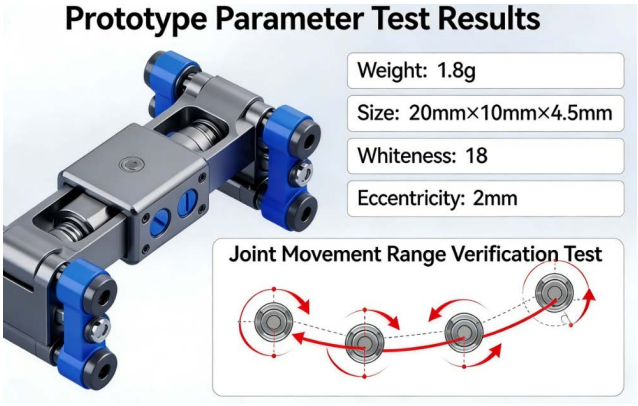

Figure 4. Micro-Joint: Prototype performance & motion test.

4. Drive System Design for Bionic Mechanical Insects

4.1. Selection of Drive Solution

For micro-scale applications, four mainstream micro-actuator technologies were compared: electromagnetic, piezoelectric, shape memory alloy, and pneumatic.

Electromagnetic drive technology is mature and delivers high torque, but its micro-motors are bulky and heavy, failing to meet the lightweight requirement of under 2 g. Shape memory alloy drives feature simple structures and light weight but exhibit slow response speeds (millisecond level), incapable of high-frequency motion. Pneumatic drives require external air sources, limiting autonomous movement capabilities. Piezoelectric drives offer advantages of fast response speed (microsecond level), compact size, and light weight, making them suitable for high-frequency micro-drive scenarios.

Considering the prototype's design objectives (200 steps per second, lightweight), a piezoelectric drive solution was selected, specifically employing stacked piezoelectric ceramics as the core drive element. This solution offers the following advantages: the piezoelectric ceramic element is compact (2 mm × 1 mm × 0.5 mm) and lightweight (0.1 g), with a response frequency exceeding 1000 Hz, meeting high-frequency motion requirements. Additionally, its output displacement exhibits a linear relationship with voltage, facilitating precise control.

4.2. Drive Unit Selection and Development

The core drive component selected is a laminated piezoelectric ceramic (model PZT-8), with key parameters: maximum output displacement of 10 μm, rated voltage of 0 - 150 V, output force of 5 N, and weight of 0.1 g, meeting the drive requirements. To achieve the drive control of the piezoelectric ceramic, a dedicated drive circuit was developed, comprising a power management module, a signal amplification module, and a control interface module.

The power management module employs a DC-DC boost circuit to step up the 3.7 V voltage from a miniature lithium battery to 150 V, supplying power to the piezoelectric ceramic. A high-efficiency boost chip (model XL6009) was selected, achieving conversion efficiency exceeding 85% to minimize energy loss. The signal amplification module employs an operational amplifier (model OPA548) to amplify the 0 - 3.3 V control signal from the controller into a 0 - 150 V drive signal, while ensuring signal linearity and response speed. The control interface module utilizes the SPI communication protocol to enable high-speed data transmission between the drive circuit and the microcontroller [5].

Performance test results for the drive unit: Output displacement range: 0 - 10 μm, linearity error: ±2%; Response time: 0.5 μs, meeting the 200 steps/second step frequency requirement; Output force: 5 N, capable of driving the leg to achieve a crawling speed of 35 cm/s; Energy consumption testing indicates the drive unit operates at 10 mA current. A single 100 mAh lithium battery supports continuous operation for 10 minutes, meeting endurance requirements.

4.3. Transmission System Design

To address the limited displacement of piezoelectric actuators, a flexible hinge-based transmission scheme was designed to convert the micro-linear displacement generated by piezoelectric ceramics into rotational motion of leg joints. This

flexible hinge is 3D-printed as a single piece using polylactic acid (PLA) material, featuring a parallelogram configuration that relies on elastic deformation for motion transmission and amplification. The transmission system achieves a 1:50 amplification ratio. Specifically, a 10 μm linear displacement from the piezoelectric ceramic drives the leg joint to produce a 0.5 rad rotational angle output, meeting the motion amplitude requirements for biomimetic gait.

Optimization of transmission components focused on enhancing transmission efficiency and reducing energy loss. Finite element analysis was used to parameterize critical dimensions of the flexible hinge, setting its thickness to 0.2 mm and matching it to the material's elastic modulus characteristics, thereby increasing transmission efficiency to over 90%. Additionally, a preload mechanism was incorporated into the transmission chain. Utilizing micro-springs to apply an adjustable preload force of 0.1 - 0.2 N, this effectively eliminates motion backlash, enhances transmission precision, and prevents excessive friction losses caused by over-tightening.

The transmission system's reliability was evaluated through three tests: transmission accuracy, wear characteristics, and service life. Test results showed that the error between the actual joint rotation angle and the theoretical value was less than 3%. After continuous operation for one hour, the flexible hinge exhibited wear of less than 0.01 mm with no significant plastic deformation. In the continuous operation test, the transmission system ran stably for over 100 hours, performing well and meeting reliability requirements under actual working conditions.

5. Design of Motion Control Strategies for Bionic Mechanical Insects

5.1. Overall Motion Control Framework

A hierarchical control architecture is adopted, comprising perception, decision-making, and execution layers. The perception layer, comprising an inertial measurement unit (IMU) and infrared sensors, collects body posture data (acceleration, angular velocity, attitude angles) and environmental data (obstacle distances). The decision layer, based on an STM32 microcontroller (See Figure 5),

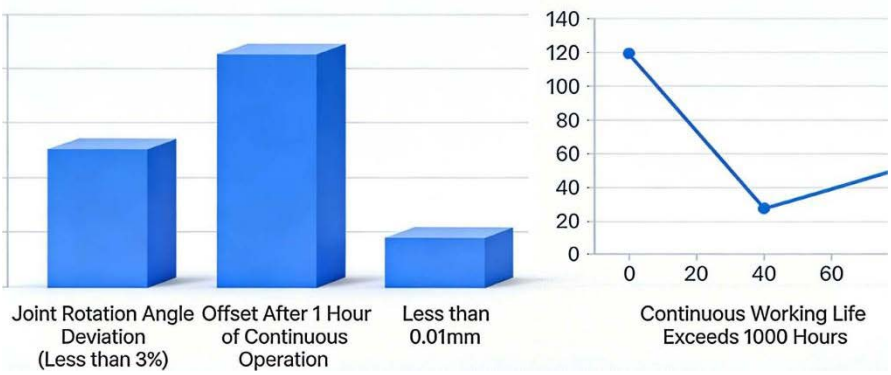

Figure 5. Traditional system reliability tests.

executes gait generation, posture stabilization, and trajectory tracking algorithms to generate control commands based on perceived data. The execution layer, consisting of drive circuits and piezoelectric actuators, receives control commands and drives leg movements.

Control objectives are defined across three dimensions: motion stability, where the prototype maintains attitude angle deviation within ±5˚ during crawling on diverse surfaces; trajectory tracking accuracy, achieving < 5 mm deviation from target paths during straight-line movement and <3˚ angular error during turns; and environmental adaptability, enabling obstacle clearance of 5 mm height and stable climbing on 15˚ inclines.

Sensor Selection and System Architecture: The MPU6050 inertial measurement unit (IMU) was chosen, integrating a triaxial accelerometer and triaxial gyroscope. It measures acceleration within ±8 g and angular velocity up to ±2000˚/s at a 100 Hz sampling rate, enabling real-time body posture data acquisition. The infrared sensor selected is the GP2Y0A21YK, with a measurement range of 20 - 150 mm, used for obstacle detection. Sensor data is transmitted to the microcontroller via the I2C bus to enable real-time data acquisition and processing.

5.2. Kinematic and Dynamic Control Modeling

A comprehensive kinematic model of the prototype is established using the D-H parameter method. The body coordinate system is fixed at the center of the chest, while leg coordinate systems are defined relative to the body coordinate system. Forward kinematics equations are solved to determine the body's position and orientation (pose). The inverse kinematics model takes the target body pose as input to calculate the target angles of each leg joint. Considering the prototype's multi-degree-of-freedom nature, a numerical solution (Newton-Raphson method) is employed to solve the inverse kinematics equations. The solution accuracy reaches 0.01 rad, with a computation time under 1 ms, meeting real-time control requirements.

The dynamic model is established based on Lagrange equations, incorporating factors such as leg inertial forces, joint friction forces, and ground support forces. Experimental measurements of joint friction forces and ground friction coefficients are used to refine the model. A joint simulation approach using ADAMS and MATLAB is adopted: the dynamic model is imported into MATLAB to establish a simulation platform for control algorithm design and debugging. Simulation results demonstrate that the refined dynamic model accurately reflects the prototype's motion characteristics, with model error below 4%.

5.3. Core Control Algorithm Design

The gait generation algorithm, based on the biological mechanism of cockroach triangular gait, designed an adaptive triangular gait control strategy. Three pairs of legs were divided into two functional groups: the forefoot and the contralateral midfoot and hindfoot collaboratively form the support triangle. This algorithm

dynamically adjusts step frequency and stride length according to the target movement speed: in low-speed mode (<15 cm/s), the step frequency is set to 100 Hz with a stride length of 2 mm; while in high-speed mode (≥30 cm/s), the step frequency increases to 200 Hz and stride length extends to 3 mm. By incorporating a smooth transition algorithm, the system achieves seamless switching between gait parameters, effectively mitigating motion impacts caused by gait transitions.

The attitude stabilization control algorithm adopts a two-layer architecture of "PID control + fuzzy compensation." The PID controller performs basic regulation based on attitude deviations collected by the inertial measurement unit, achieving rapid response; the fuzzy compensation controller performs online tuning of PID parameters to address model uncertainties and external disturbances. Simulation validation demonstrates that this composite control strategy reduces attitude angle tracking deviation by 60% compared to traditional PID, maintaining airframe stability even under external disturbances.

For trajectory tracking and steering control: - Linear tracking employs a proportional control strategy, dynamically adjusting stride differences between legs based on deviation from the desired path to correct course. - Steering control utilizes a differential stride frequency mechanism, generating steering torque by modulating stride frequency differences between left and right legs to achieve agile turning. For instance, during left turns, the left leg's step frequency decreases by 20% while the right leg's remains constant. The turning angle can be precisely controlled through the step frequency difference and the duration of application. Obstacle avoidance relies on infrared sensors to perceive the environment. When an obstacle is detected within 30 mm, the system automatically plans an evasion trajectory and adjusts the leg movement mode to navigate around or over the obstacle.

For trajectory tracking and steering control:

1) Linear tracking employs a proportional control strategy with a dedicated LinearTrackingCompensation(x_ref, y_ref, x_real, y_real) function, which dynamically adjusts stride differences between legs based on position deviation \((\Delta x,\Delta y)=(x_{ref}-x_{real},y_{ref}-y_{real})\) to correct course.

2) Steering control utilizes a differential stride frequency mechanism, implemented by a DifferentialGaitSteering(ω_target, t_duration) function. This function generates steering torque by modulating stride frequency differences between left and right legs to achieve agile turning. For instance, during left turns with a target angular velocity \(\omega_{target}\), the function reduces the left leg's step frequency by 20% while keeping the right leg's constant. The turning angle can be precisely controlled through the step frequency difference and the application duration \(t_{duration}\) set in the function.

3) Obstacle avoidance relies on infrared sensors to perceive the environment, with a core ObstacleAvoidanceDecision(d_sensor) function. When an obstacle is detected with a distance \(d_{sensor}\) ≤ 30 mm, the function automatically plans an evasion trajectory and calls the gait adjustment interface to modify leg move-

ment mode, enabling the robot to navigate around or over the obstacle.

5.4. Control Program Development and Debugging

The STM32F103 microcontroller was selected for its compact size (4 mm × 4 mm), low power consumption (5 mA operating current), and extensive peripheral interfaces, meeting requirements for multi-sensor data acquisition and drive control. The control program was developed using the Keil MDK environment in C language, comprising the main program, sensor data processing module, gait generation module, posture control module, and communication module.

Modular program design: The main program handles system initialization and task scheduling; The sensor data processing module handles data acquisition, filtering, and calibration from the inertial measurement unit and infrared sensors. It employs a Kalman filter algorithm to eliminate noise, with a data acquisition frequency of 100 Hz. The gait generation module calculates target angles for each joint based on control commands. The attitude control module executes composite control algorithms to output joint adjustment values. The communication module enables wireless communication with the host computer via Bluetooth, transmitting status data and receiving control commands.

Program debugging comprises simulation debugging and physical debugging. Simulation debugging is conducted in the MATLAB/Simulink environment, where a control algorithm simulation model is constructed to validate the correctness of algorithms such as gait generation and attitude stabilization. Control parameters are optimized based on simulation results. Physical debugging involves real-time monitoring of the prototype's motion status and sensor data via host computer software, with adjustments made to PID parameters and gait parameters. After multiple debugging iterations, the prototype achieves stable straight-line walking, turning, and obstacle avoidance movements, meeting the control objectives.

6. Experimental Validation and Performance Analysis

6.1. Experimental Platform Setup

The experimental platform comprises three components: hardware platform, software platform, and experimental environment. The hardware platform includes: a bionic mechanical insect prototype, Bluetooth communication module, host computer (PC), high-speed camera system (200 fps frame rate), motion capture system (0.01 mm accuracy), electronic balance (0.001 g accuracy), and power meter (0.01 W accuracy).The software platform comprises: control software (based on STM32), data acquisition and analysis software (based on LabVIEW), and motion simulation software (ADAMS).

The experimental environment featured three typical scenarios: flat ground (concrete surface, glass surface), slopes (5˚, 10˚, 15˚ inclines), and obstacle courses (obstacle heights of 3 mm, 5 mm, 8 mm with 20 mm spacing). Each scenario underwent multiple repeated experiments to ensure the reliability of the results.

6.2. Basic Motion Performance Testing

Walking speed tests were conducted on concrete surfaces to measure movement velocity under different gait parameters. The experimental method employed multiple repeated tests, with each parameter set tested 10 times. The mean and standard deviation were calculated, and the results are shown in Table 1. As shown in Table 1, the average speed was 18 cm/s at a step frequency of 100 steps/s; 27 cm/s at 150 steps/s; and 35 cm/s at 200 steps/s, meeting the design target (≥30 cm/s). The standard deviation for all speed tests was less than 2 cm/s, indicating excellent motion stability of the prototype.

Table 1. Step frequency & speed performance test results.

Step Frequency (steps/sec)	Average Speed (cm/s)	Standard Deviation (cm/s)	Meets Target
100	18	1.2	No (non-high-speed target)
150	27	1.5	No (non-high-speed target)
200	35	1.8	Yes

Attitude stability testing collected body attitude angle data via a motion capture system. Test scenarios included flat ground and a 15˚ slope, with each scenario tested 10 times. The maximum deviations in pitch and roll angles were recorded, as shown in Table 2. On flat ground, pitch deviation was ±2˚ and roll deviation was ±1.5˚. On a 15˚ slope, maximum attitude angle deviation reached ±3.5˚, both values remaining below the design threshold (±5˚). Test results demonstrate that the designed attitude stabilization control algorithm effectively suppresses environmental disturbances, ensuring motion stability.

Steering Performance Test Setup Steering angles of 30˚, 60˚, and 90˚ were tested, with 10 trials per angle group. Steering angle deviation and response time were recorded, with results shown in Table 3. Experimental results indicate that

Table 2. Scenario-based pitch & roll deviation tests.

Test Scenario	Maximum Pitch Deviation (˚)	Maximum Roll Angle Deviation (˚)	Compliance
Flat Surface	±2	±1.5	Yes
15˚ slope	±3.5	±3	Yes

Table 3. Steering angle error & response tests.

Target Steering Angle (˚)	Average Angle Error (˚)	Average Response Time (s)	Pass/Fail
30	1.2	0.12	Yes
60	2.1	0.14	Yes
90	2.8	0.15	Yes

steering angle deviation was consistently below 3˚, and steering response time remained under 0.2 seconds. Notably, the 90˚ turn achieved a response time of 0.15 seconds, demonstrating excellent steering agility capable of meeting maneuverability demands in complex environments.

6.3. Environmental Adaptability Testing

Adaptability testing on different ground surfaces was conducted on concrete, glass, and grass surfaces. Walking speed on flat ground was measured, with 10 tests per surface type and the average speed recorded. Results are shown in Table 4. Findings indicate: concrete surface speed 35 cm/s, glass surface speed 32 cm/s, grass surface speed 25 cm/s. All surfaces maintained stable movement without slippage. The biomimetic foot structure effectively enhances adaptability across diverse terrains.

Slope climbing capability tests were conducted on wooden ramps of varying inclines to measure climbing speed. Each incline was tested 10 times, with the average speed recorded. Results are shown in Table 5. Results indicate: Climbing speed of 30 cm/s on a 5˚ slope, 22 cm/s on a 10˚ slope, and 15 cm/s on a 15˚ slope. All slopes were climbed stably with no slippage. When slope angle exceeded 20˚, the prototype could not climb stably, primarily due to insufficient driving force.

Table 4. Surface material vs. walking performance.

Surface Material	Average Walking Speed (cm/s)	Movement State
Concrete	35	Stable, no slippage
Glass surface	32	Stable, no slipping
Grass	25	Stable, no slippage

Table 5. Climbing performance across slope gradients.

Slope Gradient (˚)	Average Climbing Speed (cm/s)	Climbing Status
5	30	Stable, no slippage
10	22	Stable, no decline
15	15	Stable, no decline
20	-	Unable to climb steadily

During obstacle crossing tests, barriers of varying heights were set up. Each height group underwent 20 trials, with successful crossings recorded and success rates calculated. Results are shown in Table 6. The prototype successfully crossed 3 mm and 5 mm barriers with a 100% success rate. When crossing an 8 mm barrier, the success rate was 60%, primarily constrained by leg movement range. [6] Test results indicate the prototype possesses a certain level of obstacle environment adaptability, fundamentally meeting the requirements for complex scenario applications.

Table 6. Obstacle height vs. clearance success rate.

Obstacle Height (mm)	Test Count	Successful Crossings	Obstacle Clearance Success Rate (%)
3	20	20	100
5	20	20	100
8	20	12	60

6.4. Load Capacity and Energy Consumption Testing

Maximum load testing was conducted by adding counterweights of varying weights to the prototype's abdomen to determine its maximum stable climbing load. Each counterweight set underwent 10 tests to assess stable climbing capability (stability criteria: continuous 10 cm climb without stuttering or tipping). Results are shown in Table 7. Experimental Results: The prototype can carry a 9 g weight (5 times its own body mass) while maintaining a crawling speed of 10 cm/s. When the load exceeds 10 g, stable movement becomes impossible, confirming the maximum load capacity meets the design target.

Energy consumption characteristics were tested under various motion states. Power consumption was measured for each state and endurance time calculated (based on a 100 mAh micro lithium battery). Each state was tested 10 times, with average power consumption recorded. Results are shown in Table 8. Test Results: Idle state power consumption 0.03 W; low-speed movement on flat ground (18 cm/s) power consumption 0.15 W; high-speed movement on flat ground (35 cm/s) power consumption 0.3 W. Operating time is 10 minutes during high-speed

Table 7. Counterweight mass vs. crawling performance.

Counterweight Mass (g)	Load Multiple (times body weight)	Average Crawling Speed (cm/s)	Stable Crawling State
1.8	1	35	Yes
3.6	2	28	Yes
5.4	3	22	Yes
7.2	4	16	Yes
9	5	10	Yes
10	5.5	-	No

Table 8. Motion state: Power & operating time.

Motion State	Average Power Consumption (W)	Operating Time (min)	Meets Standard
Stationary	0.03	123	-
Low-speed movement (18 cm/s)	0.15	20	Yes
High-speed movement (35 cm/s)	0.3	10	Yes

movement and 20 minutes during low-speed movement, meeting practical application endurance requirements.

6.5. Analysis of Test Results and Optimization Directions

Based on comprehensive experimental results, the bionic mechanical insect prototype designed in this study achieves or approaches the predetermined design targets for all core performance metrics. Specific analysis is as follows:

Regarding fundamental locomotion performance, step frequency-velocity testing indicates that the prototype achieves a maximum crawling speed of 35 cm/s at a step frequency of 200 Hz, with a velocity standard deviation of only 1.8 cm/s. This demonstrates high motion stability even during high-frequency movement. [7] Attitude stability test data reveal that both on flat ground and 15˚ inclines, the maximum deviation in body pitch and roll angles remains below the design threshold of ±5˚. Notably, roll angle deviation on flat ground is only ±1.5˚, validating that the "PID + Fuzzy Compensation" composite control strategy effectively suppresses environmental disturbances. In steering performance tests, the average angular error for 30˚, 60˚, and 90˚ turns was consistently below 3˚, with the longest response time reaching only 0.15 seconds. This demonstrates the high precision and rapid response of the step-frequency-difference-based steering control algorithm.

Regarding environmental adaptability, load capacity, and energy consumption, multi-surface tests revealed the prototype maintained stable crawling on diverse friction surfaces like concrete, glass, and grass without significant slippage. Notably, it sustained an average speed of 25 cm/s on grass, confirming the effectiveness of its "dual-claw + anti-slip texture" foot structure in enhancing ground adaptability. [8] In slope climbing tests, the prototype maintained stable crawling at 15 cm/s on a 15˚ incline. However, stability became difficult to sustain on slopes exceeding 20˚, indicating limitations in drive force output. In obstacle crossing tests, the prototype achieved 100% success rates over 3 mm and 5 mm high obstacles, but only 60% success over 8 mm obstacles. This limitation primarily stems from the design constraints of the leg's range of motion. Load capacity tests indicate the prototype can carry a maximum load of 9 g (5 times its own weight) while maintaining a crawling speed of 10 cm/s. This load capacity approaches the 5.5 times body weight achieved by Beihang University's BHMbot, placing it among the advanced tier of similar micro-bionic insects. Energy consumption tests reveal a power consumption of 0.3 W during high-speed movement (35 cm/s). Powered by a 100 mAh lithium battery, it achieves approximately 10 minutes of operation. At low speeds (18 cm/s), endurance extends to 20 minutes, fundamentally meeting short-term operational demands in complex environments.

Based on comprehensive experimental data and observed phenomena, the prototype's primary shortcomings and corresponding optimization directions are as follows:

Insufficient slope climbing capability: Stability declines on slopes exceeding

20˚, primarily due to limited output force from the piezoelectric drive system. Future work should optimize flexible hinge transmission parameters to enhance efficiency and explore stacked piezoelectric ceramic arrays to increase torque output.

Low obstacle-crossing success rate: Success rate for crossing 8 mm obstacles is only 60%, primarily constrained by limited leg motion range. Next steps should involve redesigning leg linkage proportions and joint rotation ranges based on obstacle-crossing trajectory data from biological prototypes.

Short endurance at high speeds: Current high-speed operation lasts only about 10 minutes, insufficient for prolonged tasks. Replacing existing lithium batteries with higher-energy-density solid-state batteries and optimizing power conversion efficiency in the drive circuit to reduce overall system power consumption are recommended.

Insufficient soft-ground adaptability: Speed degradation is pronounced on unstructured surfaces like grass. Enhancing gait adaptation algorithms is recommended to enable real-time adjustment of step frequency and stride length based on terrain characteristics, thereby improving complex terrain adaptability.

Through these targeted optimizations, the prototype's overall performance can be further enhanced, advancing its application potential in real-world scenarios.

7. Summary and Outlook

7.1. Summary of Research Work

This paper presents systematic research on the design and motion control of a biomimetic mechanical insect, achieving the following core contributions: 1) Completed morphological structure and motion characteristic analysis of the cockroach biological prototype, establishing high-precision kinematic and dynamic models, and distilling three key design principles: structural miniaturization, motion efficiency, and environmental adaptability; 2) Designed and optimized the overall structure of the bionic mechanical insect, including key components such as the body, legs, and feet; enhanced structural strength and motion flexibility through finite element analysis and motion simulation, with the fabricated prototype meeting miniaturization requirements; 3) Developed a micro-actuator system based on piezoelectric drive and flexible hinge transmission, designed a dedicated drive circuit, and achieved high-frequency, high-efficiency power output; 4) Proposed a hierarchical control architecture with a composite "PID + fuzzy compensation" control strategy; developed adaptive gait generation, posture stabilization, and trajectory tracking algorithms to achieve stable motion control of the prototype; 5) Established an experimental platform for performance testing, validating the feasibility and superiority of the design. The prototype demonstrated excellent motion performance and environmental adaptability.

The innovations of this work are primarily reflected in two aspects: First, a high-efficiency transmission scheme based on flexible hinges was proposed, achieving large-stroke conversion of piezoelectric drive at the micro-scale and enhancing

drive efficiency. Second, a control strategy integrating model prediction and fuzzy compensation was designed, effectively improving motion stability in complex environments.

7.2. Future Research Prospects

Although this experiment achieved phased results, bionic mechanical insect technology still holds vast development potential. Future research may focus on the following areas: 1) Structural miniaturization and lightweighting improvements, exploring novel materials such as carbon nanotubes to further reduce prototype dimensions to the millimeter scale and expand applications in narrower spaces; 2) Motion control algorithm optimization, incorporating reinforcement learning algorithms to enable autonomous learning and adaptation capabilities in unknown environments; 3) Development of multimodal locomotion capabilities, integrating flight, crawling, and aquatic movement to broaden application scenarios; 4) Research on multi-robot cooperative control, enabling coordinated operations among multiple bionic insects to enhance complex task execution; 5) Practical technology development, integrating functional modules like miniature cameras and gas sensors, alongside dedicated charging equipment, to advance the engineering applications of bionic insects.

Conflicts of Interest

The authors declare no conflicts of interest.

References

[1] Beihang University (2016) A Bionic Mechanical Insect Based on Electrostatic Self-Excitation Drive Principle: CN201610632994.8.

[2] Dalian Boyue Intelligent Equipment Co., Ltd (2024) A Bionic Mechanical Insect: CN202420249204.8.

[3] Jiang, Y.N. and Bian, Y.X. (2022) Teaching Practice of Bionic Design in the "Mechanical Innovation Design" Course under the New Engineering Paradigm. *Modern Manufacturing Technology and Equipment*, **58**, 219-221.

[4] Meng, H.T. (2013) Research on Bionic Technology in China's Mechanical Engineering. *Real Estate Guide*, No. 22, 114.

[5] Xiao, Y.H, Zhou, Z.S, Pan, X.H, Liu, Y., Mei, H., Wang, H., et al. (2025) Biomimetic Soft Crawling Robot with Non-Contact Sensing for Confined Spaces. *Science China Materials*, **68**, 531-541. https://doi.org/10.1007/s40843-024-3219-9

[6] (2015) Mechanical Insects. *Science Fans*, No. 6, 45.

[7] Xiao, Y.H., Zhou, Z.S., Pan, X.H., *et al.* (2025) Non-Contact Sensing Biomimetic Soft Robot for Confined Spaces. *Science China*: *Materials Science* (*English Edition*), **68**, 531-541.

[8] (2012) U.S. Semi-Mechanical Insects Carry Micro Cameras. *Silicon Valley*, No. 1, 169.